

Stability of a planar-defect structure of the wurtzite AlN ($10\bar{1}0$) surface: Density functional study

Honggang Ye, Guangde Chen, Yelong Wu, and Youzhang Zhu

Non-equilibrium Condensed Matter and Quantum Engineering Laboratory, The Key Laboratory of Ministry of Education, School of Science, Xi'an Jiaotong University, Xi'an 710049, People's Republic of China

Su-Huai Wei

National Renewable Energy Laboratory, Golden, Colorado 80401, USA

(Received 28 February 2009; published 10 July 2009)

The formation energy of a structure is usually increased by the appearance of a defect. A stoichiometric planar defect structure of the wurtzite AlN ($10\bar{1}0$) surface, however, is found to be lower in energy than the ideally truncated surface by first-principles calculations. The intriguing phenomenon is directly attributed to the large scale surface relaxation induced by the defect structure and the intrinsic reason is pointed to the strong ionicity and small c/a (lattice constant ratio) of AlN. A suggested growth mode shows that the defect surface structure is compatible with the growth of the correct wurtzite AlN film on the ($10\bar{1}0$) plane.

DOI: [10.1103/PhysRevB.80.033301](https://doi.org/10.1103/PhysRevB.80.033301)

PACS number(s): 68.35.Dv, 61.46.Km, 73.20.At

AlN is usually partially regarded as a wide band gap semiconductor which has potential applications in ultraviolet emitters, lasers, and high-mobility transistors, and partially regarded as a substrate or buffer layer for the growth of III-nitrides and their alloys.¹⁻⁴ Many of these applications are related to surface properties; study of the AlN surface is thus necessary. Theoretical study of the AlN nonpolar ($10\bar{1}0$) surface is insufficient comparing to the well-studied polar (0001) and (000 $\bar{1}$) surfaces.⁵⁻⁷ Works on it are merely limited to the clean surface.^{8,9} However, it plays an important role for AlN. Much attention has been paid to the epitaxial growth of AlN films on the ($10\bar{1}0$) plane to avoid the large polarization field in polar film.^{10,11} Detailed study of the ($10\bar{1}0$) surface structure is helpful to understand the mechanism of film growth and the formation of some defects. The ($10\bar{1}0$) surface is also generally reported to be the main component of the lateral facets of AlN nanowires and nanotubes.¹²⁻¹⁴ Study of the surface property is especially important for these nanoscale materials.

In this Brief Report, a stoichiometric planar defect surface (PDS) structure of the wurtzite AlN ($10\bar{1}0$) surface is studied by first-principles methods. It is interesting that our calculation outcomes reveal that the PDS is lower in energy than the ideal AlN ($10\bar{1}0$) surface. It thus should be the general structure of the AlN ($10\bar{1}0$) surface. However, this phenomenon does not occur for GaN and InN.¹⁵ The origin is explored and a growth mode is suggested to show that the PDS does not influence the growth of the correct wurtzite AlN film on the ($10\bar{1}0$) plane.

The wurtzite ($10\bar{1}0$) surface is characterized by cation and anion dimers, as shown in Fig. 1(a), with one dimer in each unit cell. The PDS structure concerned in this work is shown in Fig. 1(b). It can be constructed by exchanging the Al and N atoms in the top two layers of the ($10\bar{1}0$) surface and translating them along the [0001] direction by $c/2$. The PDS structure does not involve any error bonds except for the variations in bond angles. The structure feature that should

be noted is that the top view of the PDS is the same as that of the ideal ($10\bar{1}0$) surface. Variation can only be seen from the side view, in which the original sixfold rings become fourfold and eightfold rings.

The density functional theory calculations are performed within the generalized gradient approximation of Perdew and Wang¹⁶ as implemented by the Vienna *Ab initio* Simulation Package code.^{17,18} The Vanderbilt ultrasoft pseudopotentials (USPP)¹⁹ are generally used in this work, but the interaction between the core and the valence electrons are also treated

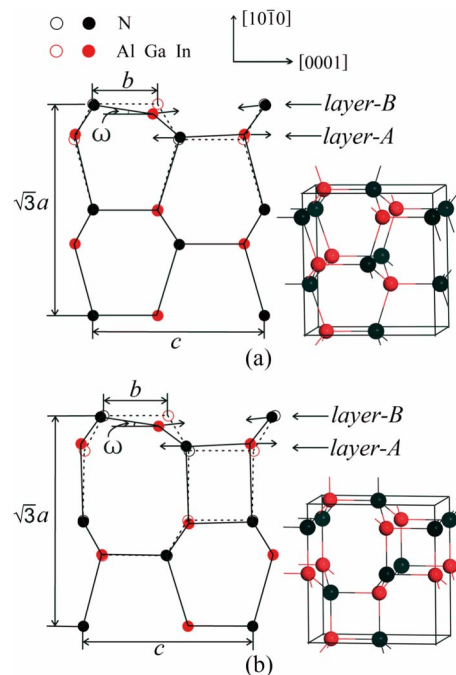


FIG. 1. (Color online) Schematic representations of the relaxed (filled circles) and unrelaxed (empty circles) atomic positions of (a) ideal and (b) defect ($10\bar{1}0$) surface. The black and red circles represent anions and cations, respectively. The arrows denote possible transformation process between the two structures. The inserts are the three-dimensional views of the unit cell of surface models.

TABLE I. Structure and formation energy comparison between the PDS and ideal AlN ($10\bar{1}0$) surface. ω and Δb denote the top layer bond rotation angle and relative bond constriction, respectively. The data are generally obtained with USPP except for these in parentheses which are computed with PAW method.

	ω ($^\circ$)	Δb (%)	energy [eV/(1×1)]
AlN (defect)	8.1 (8.8)	8.1 (8.1)	2.135 (2.113)
AlN (ideal)	6.3 (6.8)	7.3 (7.3)	2.145 (2.120)
GaN (defect)	7.8	8.6	1.710
GaN (ideal)	7.2	8.4	1.658
InN (defect)	8.0	7.3	1.669
InN (ideal)	6.4	6.9	1.604

with the projector augmented wave (PAW)²⁰ method to confirm some results. The energy cutoff for the basis function is 500 eV for AlN and 700 eV for GaN and InN. We employ Monkhorst-Pack sampling scheme with k -point mesh of $5 \times 8 \times 1$.²¹ The slab models are built containing 16 atomic layers with 12 Å vacuum space separating the slabs. The top four layers at both sides of the slabs are allowed to relax by minimizing the quantum mechanical force on each ion site to be less than 0.01 eV/Å. The other layers are fixed in the optimized bulk configuration. Test calculations show that the cell size is converged.

Relaxation of the ideal ($10\bar{1}0$) surface of III-nitrides has been well studied.^{9,22,23} The top layer bond rotation angle ω and bond constriction Δb are usually used to characterize the relaxation magnitude. It can be seen from the representations shown in Fig. 1 and the data given in Table I that the PDS follows the same relaxation mode as the ideal ($10\bar{1}0$) surface, but both ω and Δb of the PDS for all the three semiconductors are larger. This result can be understood from the symmetry of the defect structure. Each four atomic layers can be regarded as a unit cell of the ($10\bar{1}0$) surface model, the three-dimensional view for which is inserted in Fig. 1(a). If the top four layers of the PDS model are also treated as a unit cell, the three-dimensional view for which is inserted in Fig. 1(b), it has the same atomic configuration along the $[10\bar{1}0]$ and $[0001]$ directions, but the lengths of the initially constructed model are $\sqrt{3}a$ and c , respectively, along the two directions. Because the c/a is usually smaller than $\sqrt{3}$, the PDS tends to expand in the $[0001]$ direction and large compressive stress is induced, which makes the relaxation magnitude of the PDS is larger than that of the ideal one. Moreover, the c/a of both GaN(1.630) and InN(1.618) are larger than that of AlN(1.603), closer to $\sqrt{3}$, so the discrepancies in relaxation magnitude between the PDS and the ideal surface for GaN and InN are less than that for AlN.

The formation energies of the ideal and the defect ($10\bar{1}0$) surfaces for AlN, GaN, and InN are also given in Table I. It is interesting that the PDS for AlN is 10 meV lower in energy than the ideal one. This result disobeys the general idea

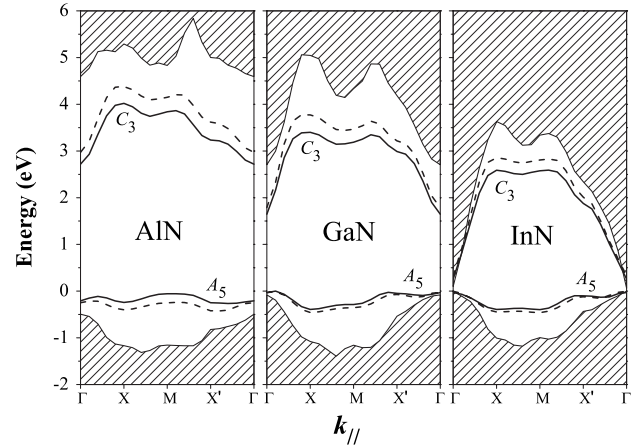


FIG. 2. Electronic band structures of the ideal and planar defect ($10\bar{1}0$) surfaces for AlN, GaN, and InN. The shaded region corresponds to the bulk projected band structure. The solid (dashed) lines present the surface states of the ideal (defect) surface. A_5 is an N-related occupied band and C_3 is a cation-related empty band.

that the appearance of a defect will increase a structure's formation energy. Calculations are performed again with the PAW method to validate this result and consistent consequences are obtained by the two methods. The intriguing phenomenon can be understood from two aspects. On one hand, the formation energy of the PDS model is increased by the undesired bond angles induced by the defect structure. On the other hand, it is decreased by the large scale surface relaxation (compared to that of the ideal surface). The energy decrease due to surface relaxation can be certified from the downward shift of the occupied N-related A_5 band in Fig. 2, although the ion-ion interaction is not included here. The final result depends on which of the two contrary aspects is stronger. The calculation outcomes indicate that the decreasing effect is stronger for AlN.

In the cases of GaN and InN, the formation energies of PDS, however, are 52 and 65 meV higher than those of the responding ideal surfaces. This result is consistent with a previous report¹⁵ but contrary to that for AlN. It can be also understood from the above two aspects affecting energy. According to Pauling's ionicity scale,²⁴ GaN(0.486) and InN(0.496) are more covalent than AlN(0.550), so the bond energies of GaN and InN are more sensitive to bond angles, and the energy increased by the undesired bond angles is larger. On the other hand, because the discrepancies in relaxation magnitude between the PDS and the ideal surface for GaN and InN are small, the energy decrement due to surface relaxation is less, as shown by the obscure downward shift of the A_5 band in Fig. 2. Hence the energy increment is larger than the decrement for GaN and InN. We can further conclude that the intrinsic origin of this intriguing phenomenon which occurs only for AlN is the strong ionicity and small c/a of AlN based on the two factors affecting energy.

The ($10\bar{1}0$) surface can also appear as the lateral facets of the AlN nanowire, so calculations are performed for AlN nanowires with ideal and planar defect lateral facets, respectively, to do a further verification of our result. As shown in Fig. 3, the difference in the top views of their cross sections

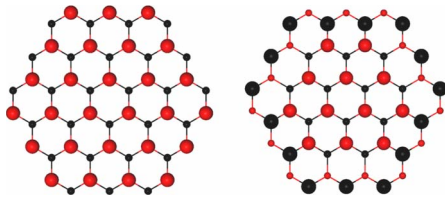


FIG. 3. (Color online) Top views of the cross section of AlN nanowires along the $[0001]$ direction, whose lateral surfaces are composed by six ideal (left) and planar defect (right) $(10\bar{1}0)$ planes, respectively. The black and red balls represent N and Al atoms, and their size difference denotes the atoms are in first (large) or second (small) layer.

is that a uniform Al or N plane is seen for the ideal AlN nanowire, but the atoms at the edge and interior are different for the defect one. Periodic models are built with 10 \AA lateral vacuum space separating the nearest two ones. The unit cell is one c long, containing 108 atoms. The lateral area of each nanowire is about 18 times of the area of (1×1) $(10\bar{1}0)$ surface. After full relaxation, the formation energy of the nanowire with defect lateral surface is 250 meV lower than that of the ideal one. Our result, therefore, is confirmed again. Because the surface stress can be further released on the small nanowire, the energy discrepancy here is over 18 times larger than that of the $(10\bar{1}0)$ surface primitive cell.

It can be concluded from the above discussion that the PDS should be the general structure of the AlN $(10\bar{1}0)$ surface. However, another problem rises at the same time, which is how the correct wurtzite AlN film is grown on the $(10\bar{1}0)$ plane. Surface relaxation is the origin of energy decrease for the PDS, but the relaxation mainly occurs on the surface layer. So we can predict that when additional atoms are adsorbed on the defect surface, large scale relaxation will disappear and the defect structure will not be energy favorable. This prediction is validated by our calculations. When N, Al atom, or AlN layer is adsorbed, the formation energy of PDS is 306, 208, or 280 meV/ (1×1) higher than that of the ideal surface. The growth periodicity of the $(10\bar{1}0)$ film includes two atomic layers, which are marked by *layer A* and *layer B* in Fig. 1 (the *layer A* ended surface is unstable because it contains two times higher density of dangling bond).

The adsorption of *layer A* retrieves the correct wurtzite film from the defect structure. The adsorption of *layer B* makes the planar-defect structure relapse. The possible process of structure transformation is marked by arrows in Figs. 1(a) and 1(b). Repeating in this way, the planar-defect structure always appears at the *layer B* ended surface, but it does not influence the growth of the correct wurtzite AlN film on the $(10\bar{1}0)$ plane. However, it is a pity that this defect $(10\bar{1}0)$ surface structure has not been reported in experiment as far as we know. The reason might be that the PDS has the same top view as the ideal surface, which makes it hard to be seen in the experiment. We hope that it will be found from a high-resolution view of the cross section of the AlN nanowire.

An important problem with the AlN polar film is the general appearance of high density extended defects, many of which are related to the $(10\bar{1}0)$ plane.^{25,26} Previous reports suggest that the epitaxial growth of III-nitrides on the substrate of sapphire and SiC follows the three-dimensional island growth mode but not the two-dimensional layer-by-layer mode because of a large lattice mismatch.^{27,28} The planar-defect $(10\bar{1}0)$ surface may be an important component of the subgrain lateral surface. It disables perfect junction of the subgrains and an extended defect is thus produced.

In conclusion, the planar defect AlN $(10\bar{1}0)$ surface concerned in this Brief Report is energetically stable. The intriguing phenomenon is directly attributed to the large scale surface relaxation induced by the defect structure, and the intrinsic reason is the strong ionicity and small c/a of AlN. The PDS thus should be the general structure of the AlN $(10\bar{1}0)$ surface. The suggested growth mode shows that the defect-surface structure is compatible to the growth of the correct wurtzite AlN film on $(10\bar{1}0)$ plane. The general appearance of extended defects in the AlN polar film may be also related to the defect structure of the AlN $(10\bar{1}0)$ surface.

The authors gratefully acknowledge the financial support of China National Natural Science Fund (Grant No. 10474078) and the computing support of the “Intelligent Information Processing and Computing Laboratory” of XJTU. The work at NREL is supported by the U.S. DOE under Contract No. DE-AC36-99GO10337.

¹R. Songmuang, O. Landre, and B. Daudin, Appl. Phys. Lett. **91**, 251902 (2007).

²Q. Sun *et al.*, J. Appl. Phys. **104**, 043516 (2008).

³D. G. Zhao, J. J. Zhu, Z. S. Liu, S. M. Zhang, H. Yang, and D. S. Jiang, Appl. Phys. Lett. **85**, 1499 (2004).

⁴S. Raghavan, X. J. Weng, E. Dickey, and J. M. Redwing, Appl. Phys. Lett. **87**, 142101 (2005).

⁵T. Mattila and R. M. Nieminen, Phys. Rev. B **54**, 16676 (1996).

⁶H. Ye, G. Chen, Y. Zhu, and S.-H. Wei, Phys. Rev. B **77**, 033302 (2008).

⁷J. E. Northrup, R. Di Felice, and J. Neugebauer, Phys. Rev. B

55, 13878 (1997).

⁸R. Pandey, P. Zapol, and M. Causà, Phys. Rev. B **55**, R16009 (1997).

⁹A. Filippetti, V. Fiorentini, G. Cappellini, and A. Bosin, Phys. Rev. B **59**, 8026 (1999).

¹⁰R. Armitage, J. Suda, and T. Kimoto, Appl. Phys. Lett. **88**, 011908 (2006).

¹¹B. A. Haskell, S. Nakamura, S. P. DenBaars, and J. S. Speck, Phys. Status Solidi B **244**, 2847 (2007).

¹²Q. Zhao, H. Z. Zhang, X. Y. Xu, Z. Wang, J. Xu, D. P. Yu, G. H. Li, and F. H. Su, Appl. Phys. Lett. **86**, 193101 (2005).

- ¹³Y. L. Wu, G. D. Chen, H. G. Ye, Y. Z. Zhu, and S.-H. Wei, *J. Appl. Phys.* **104**, 084313 (2008).
- ¹⁴L. Zhang, J. J. Shi, and T. L. Tansley, *Phys. Rev. B* **71**, 245324 (2005).
- ¹⁵D. Segev and C. G. Van de Walle, *Surf. Sci.* **601**, L15 (2007).
- ¹⁶J. P. Perdew and Y. Wang, *Phys. Rev. B* **45**, 13244 (1992).
- ¹⁷G. Kresse and J. Furthmüller, *Comput. Mater. Sci.* **6**, 15 (1996).
- ¹⁸G. Kresse and J. Furthmüller, *Phys. Rev. B* **54**, 11169 (1996).
- ¹⁹D. Vanderbilt, *Phys. Rev. B* **41**, 7892 (1990).
- ²⁰G. Kresse and D. Joubert, *Phys. Rev. B* **59**, 1758 (1999).
- ²¹J. D. Pack and H. J. Monkhorst, *Phys. Rev. B* **16**, 1748 (1977).
- ²²U. Grossner, J. Furthmüller, and F. Bechstedt, *Phys. Rev. B* **58**, R1722 (1998).
- ²³H. G. Ye, G. D. Chen, Y. L. Wu, Y. Z. Zhu, and S.-H. Wei, *Phys. Rev. B* **78**, 193308 (2008).
- ²⁴L. Pauling, *The Nature of The Chemical Bond*, 3rd ed. (Cornell University Press, Ithaca, 1960).
- ²⁵Y. Tokumoto, N. Shibata, T. Mizoguchi, M. Sugiyama, Y. Shimogaki, J. S. Yang, T. Yamamoto, and Y. Ikuhara, *J. Mater. Res.* **23**, 2188 (2008).
- ²⁶R. Datta, C. McAleese, P. Cherus, F. D. G. Rayment, and C. J. Humphreys, *Phys. Status Solidi C* **5**, 1743 (2008).
- ²⁷V. Potin, P. Ruterana, G. Nouet, R. C. Pond, and H. Morkoc, *Phys. Rev. B* **61**, 5587 (2000).
- ²⁸X. H. Wu, P. Fini, E. J. Tarsa, B. Heying, S. Keller, U. K. Mishra, S. P. DenBaars, and J. S. Speck, *J. Cryst. Growth* **189–190**, 231 (1998).